POROSITY AND PERMEABILITY EVALUATION OF PERVIOUS CONCRETE USING THREE-DIMENSIONAL X-RAY COMPUTED TOMOGRAPHY

A JAGADEESH [1], G PING ONG[1]* and Y SU[2]

[1]Department of Civil and Environmental Engineering, National University of Singapore, 117576, Singapore
[2]Department of Civil Engineering, National Kaohsiung University of Applied Sciences, Sanmin, Kaohsiung 80778, Taiwan
*Tel: +65-6516-2279; Email: ceeongr@nus.edu.sg

ABSTRACT

The functional performance of pervious concrete pavement surfaces (such as hydraulic, acoustic and frictional performances) is greatly influenced by the design of the pervious concrete mixture and its internal pore structure. With the advancement in computational imaging technologies, it is now possible to adopt X-ray computed tomography techniques to determine the internal pore structures of pervious concrete pavement surfaces. This paper examines the use of medical three-dimensional X-ray computed tomography (CT) to determine the effective porosity and the permeability in pervious concrete pavement surfaces. X-ray CT scans on different pervious concrete pavement specimens are performed and various tomographic reconstruction algorithms are tested to evaluate the performance in estimating effective porosity and permeability in pervious concrete. Our finding is that such techniques are capable of providing a non-destructive interpretation on pervious concrete mix effective porosity and permeability with potential applications in pervious concrete mix design.

1. INTRODUCTION

Porous pavements are widely used nowadays to minimize the storm water run-off, wet weather accidents, and tire/road noise by improving the intrinsic permeability, wet pavement skid resistance, and acoustic absorption coefficients. The Association of Japan Highway (1996) reported an 80% reduction in the wet weather accidents when porous pavement surfaces were used. The usage of porous pavements results in the tire/road noise reduction of 3 to 5 dB (Berengier et al., 1997). These benefits result from the characteristics of the porous pavement internal structure such as porosity, tortuosity, permeability and pore size distribution.

Pervious concrete is a special class of hydraulic cement concrete proportioned with sufficient interconnected voids that result in a highly permeable material, allowing water to readily pass. (ACI, 2010). The amount of isolated voids within the porous concrete layer is minimal because of the usage of uniform single sized coarse aggregates in the mixture. The increasing use of pervious concrete mixtures as the functional performance layers necessitates the understanding of pore network properties and their relationships.

With the advancement in computational efficiency, there are few research studies exploring the permeability of pavement materials using X-Ray computed tomography and fluid flow simulations. Kutay at al., (2007) developed the fluid flow simulation model for the hot mix asphalt pore structure using X-Ray CT scanning and Lattice Boltzmann method. Masad et al., (2007) computed the permeability tensor coefficients of asphalt concrete using the microstructure simulation of fluid flow. Gruber et al., (2012) studied the anisotropic hydraulic conductivity, pore size distribution, ice formation in the pores using the internal pore structure obtained from CT scanning. The study of pore network parameters such as effective porosity, tortuosity, pore size determination and so on can be found in the works of Kuang et al., (2015), Sanslone et al. (2008), Chandrappa and Biligiri (2017), Coleri et al. (2012), etc.

In recent years, significant efforts have been made in the digital image processing to improve the segmentation algorithms. One of the major difficulties in the usage of X-Ray CT image processing is the determination of thresholds, which separates the air voids from the solid phase. The difficulty in the image threshold segmentation of pavement materials has been described in one of the pioneering works by Masad et al. (1999). Abera et al., (2017) examined the effectiveness of various segmentation algorithms for porous media using void ratio. Zelelew and Papagiannakis (2011) obtained the threshold by matching the laboratory proportion of each material to the image segmentation proportions. The selection of thresholds has a significant influence on the final results of the simulation model. Therefore, this paper analyses the effect of different segmentation algorithms on the pore network properties using the finite volume based fluid flow simulation model.

2. MATERIALS

Two different pervious concrete mixtures were produced in the laboratory with the siliceous aggregates of 9.5mm nominal maximum aggregate size (NMAS). The specific gravity and the percent absorption of the aggregates were found to be 2.64 and 1.35% respectively. ASTM Type I cement was used as the binding agent. A superplasticizer of 0.5% by weight of cement was added to improve the workability of the porous concrete mixtures. Pervious concrete specimens of 150mm diameter and 250mm height were prepared and cured for 28 days. The pervious concrete mixture P1 represents coarse aggregates passing through 9.5mm sieve and retained on 4.75 sieve and P2 represents coarse aggregates passing through 12.5mm sieve and retained on 9.5mm sieve.

1. METHODOLOGY

1.1 X-Ray Computed Tomography and Image segmentation

The Somatom Emotion 16-channel X-Ray CT scanner with 110kV energy was used to obtain the internal structure of the pervious concrete specimens and the setup is shown in Fig.1. A total of 300 section images of pixel size 1024 x 1024 were obtained at the interval of 0.7mm. The CT scan images are obtained in the 16-bit greyscale colour intensities varying from 0 to 65535 and is shown in the Fig.2. Filtering of images was carried out to reduce the noise using convolution kernel. The Simpleware ScanIP software was used in the conversion of scanned images to the finite volume meshes. Thresholding of air voids based on the grey scale intensities was carried out using commonly used segmentation algorithms in the pavement materials research such as Otsu's algorithm and volumetric global minima algorithm for the permeability evaluation of the pervious concrete specimens. The global

image segmentation algorithm divides the image pixels into several classes by using threshold intensity values. Following section briefly discuss the above-mentioned thresholding algorithms.

- Otsu algorithm (Otsu et al. (1979)):
  In Otsu's algorithm, the optimal thresholds are obtained by minimising the weighted within class variance or maximising the between class variance of the foreground and background classes in the image histogram. The objective function for the bi-level Otsu's algorithm is given by

$$\sigma_b^2 = w_0(\mu_0 - \mu_T)^2 + w_1(\mu_1 - \mu_T)^2 \quad (1)$$

  Where σ_b^2 is the between class variance, w_0 and w_1 are the total probabilities of intensities in each class,μ_0, μ_1 are the mean value of intensities in each class and $\mu_T$is the mean value of intensities in the total histogram. The above objective function can be easily extended for the tri-level Otsu's algorithm. In this study, both bi-level and tri-level Otsu's algorithm has been used to study the air voids in the internal structure of porous concrete.

- Volumetric based global minima algorithm (Zelelew and Papagiannakis (2011)):
  In this method, the threshold of air voids is obtained by minimising the global minima error of the experimental and image-based interconnected air void content. This method requires the laboratory determination of the percentage of interconnected air voids.

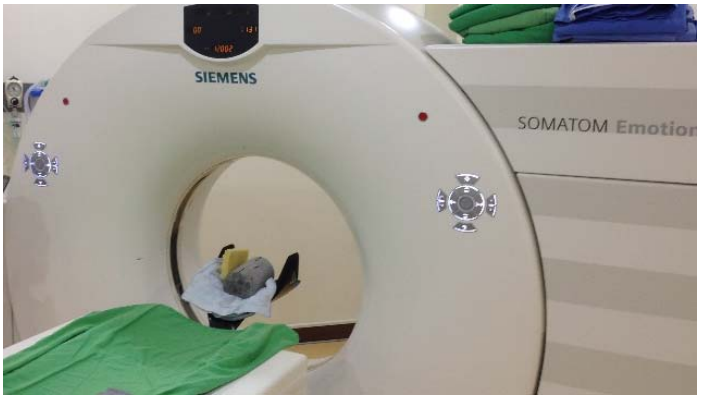

Fig.1: Scheme of medical X-Ray CT scan with test sample

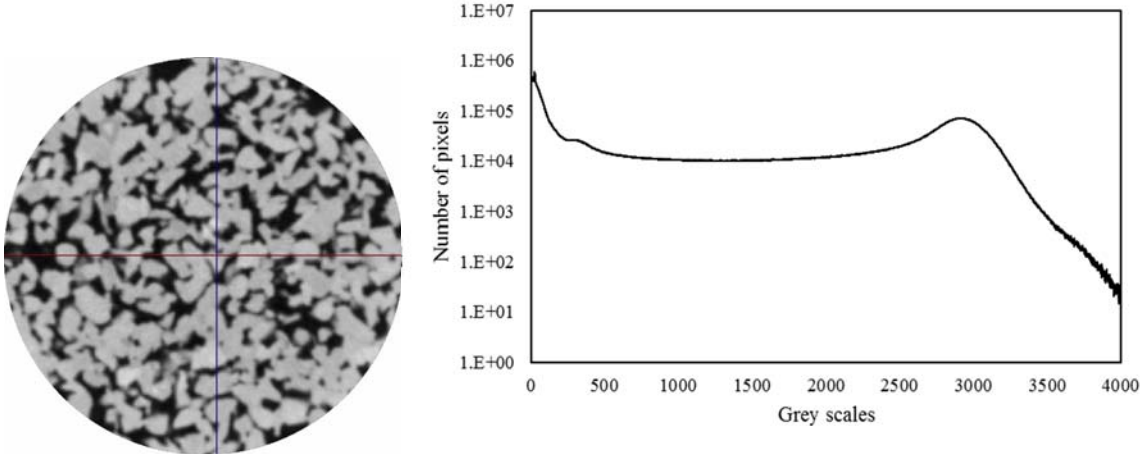

Fig.2: 2D sliced raw image of pervious concrete and its grey scale histogram

1.2 Constant head permeability test

Permeability of the pervious concrete samples was measured using the constant head permeameter in accordance with Association of Japan Highway (1996) Guide. Fig.3 shows the actual setup of the constant head permeameter. The apparatus consists of a cylinder of diameter 150 mm with the constant upstream head during the test and an outlet valve in the container with the constant downstream head. The pervious concrete samples were preconditioned in the water bath for 2 hours. The discharge measurements are made after 120 seconds of water flow through the sample to ensure the steady-state outflow. The permeability coefficient of the specimen was determined using the equation (2)

$$k_T = \frac{LQ}{hAt} \tag{2}$$

Where L = height of the specimen (mm), Q = volume of outflow water collected (mm^3), h = constant head (mm), A = cross sectional area (mm^2), t = time taken (15 seconds). The percentage of interconnected air voids or effective porosity in the pervious concrete mixtures were assessed using the equation (3)

$$n_{eff} = 1 - \frac{W_2 - W_1}{\rho_w V} \tag{3}$$

where W_1 and W_2 are the weight of the sample in water and in surface dry condition, ρ_w is the density of the water and V is the bulk volume of the sample, including the solid and void components.

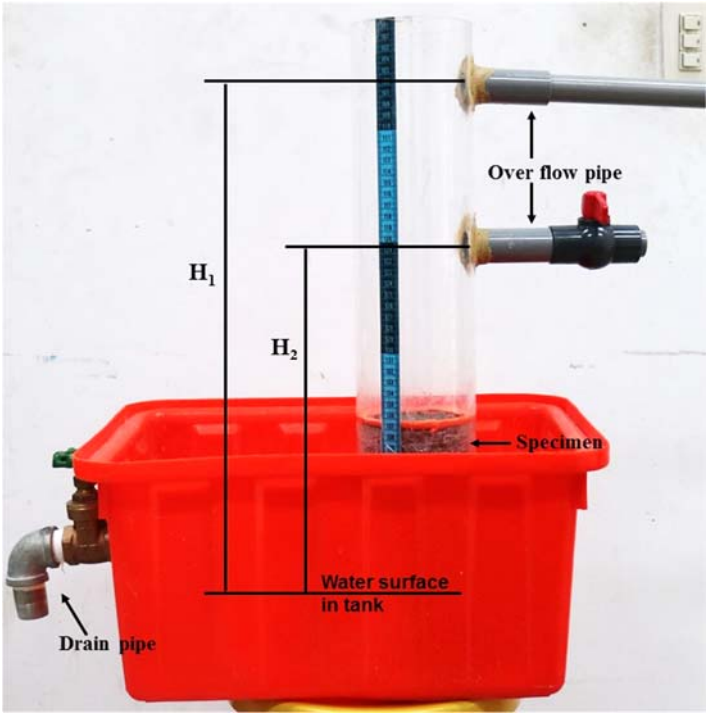

Fig.3: Actual setup of constant head permeameter

1.3 Permeability simulation model

A numerical simulation of constant head permeability test has been performed on the air voids of the pervious concrete specimens obtained from Simpleware software. Fluid behaviour in the porous media was modelled through the Navier

Stokes equations and k-ε turbulence equations in ANSYS CFX 18.1. Standard properties of the water at 25°C are adopted here. The density and dynamic viscosity of the water is taken as 998kg/m^3 and 8.899x10^{-4}kg/ms respectively. The continuity and momentum equations are:

$$\frac{\partial \rho}{\partial t} + \nabla \cdot (\rho U) = 0 \tag{4}$$

$$\frac{\partial \rho U}{\partial t} + \nabla \cdot (\rho U \otimes U) = -\nabla p' + \nabla \cdot \left((\mu + C_\mu \rho \frac{k^2}{\varepsilon})(\nabla U + (\nabla U)^T) \right) + S_M \tag{5}$$

where S_M is the sum of body forces, p' is the modified pressure. The turbulent kinetic energy k and turbulent eddy dissipation ε are obtained from the differential transport equations:

$$\frac{\partial (\rho k)}{\partial t} + \nabla \cdot (\rho U k) = \nabla \cdot \left[\left(\mu + \frac{\mu_t}{\sigma_k} \right) \nabla k \right] + P_k + P_{kb} - \rho \varepsilon \tag{6}$$

$$\frac{\partial (\rho \varepsilon)}{\partial t} + \nabla \cdot (\rho U \varepsilon) = \nabla \cdot \left[\left(\mu + \frac{\mu_t}{\sigma_\varepsilon} \right) \nabla \varepsilon \right] + \frac{\varepsilon}{k} (C_{\varepsilon 1} (P_k + P_{\varepsilon b}) - C_{\varepsilon 2} \rho \varepsilon) \tag{7}$$

Where $C_{\varepsilon 1}, C_{\varepsilon 2}$, σ_k and σ_ε are model constants, P_{kb} and $P_{\varepsilon b}$ represent buoyancy turbulence and P_k represent turbulence production due to viscous forces.

A representative elementary volume of 100mm X 100mm X 100mm was taken from the truncation of an initial pervious concrete cylinder. A constant pressure difference between the inlet and outlet surfaces was maintained in the simulation. A mesh convergence study was performed and it was revealed that 2.5 million fluid elements are required to provide sufficiently reliable results. Fig.4 shows the pore network structure of one of the test samples along with the applied boundary conditions.

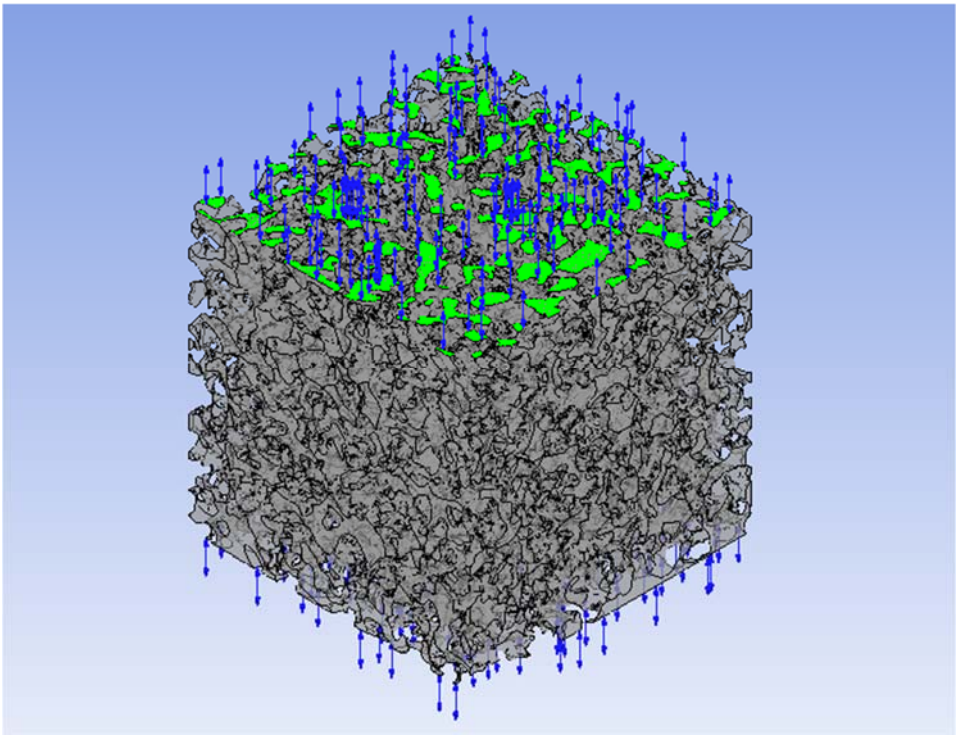

Fig.4: Pore network structure of pervious concrete with boundary conditions

2. RESULTS AND DISCUSSION

The three thresholding techniques described in the previous section were applied to X-Ray CT scan images of two different pervious concrete mixtures. The air void threshold for the sample P1 using the segmentation algorithms such as Otsu's bi-level, tri-level and volumetric algorithms was found to be 1678, 1471 and 1647 respectively and the segmented slices are shown in Fig.5. The threshold values for the sample P2 was found to be 1792, 1168 and 1694 respectively.

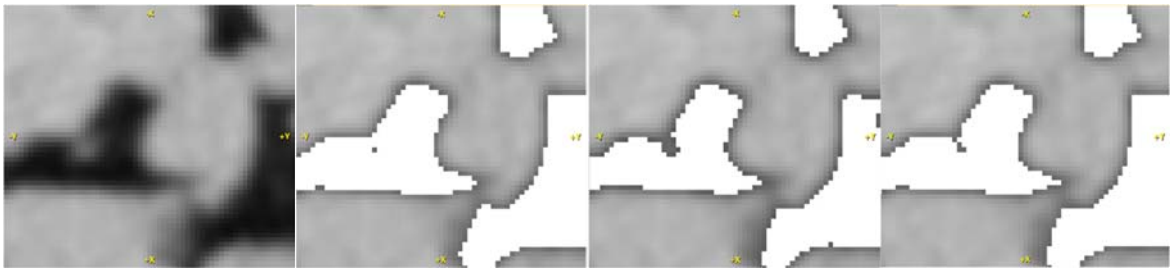

Fig.5: Comparison of original image (magnified for a single pore) with different thresholding methods applied (a) original image; (b) Otsu's bi-level; (c) Otsu's tri-level; (d) Volumetric method

2.1 Discharge characteristics

The fluid flow simulations were conducted for the reconstructed 3D images of pervious concrete mixtures with various segmentation algorithms and the results are shown in the Fig.6. Experimental results show that as the nominal maximum size of the aggregates in the porous concrete mixture increases, an increase of geometric dimensions of the pore network and hence the increase of vertical permeability is observed. It can be seen that the increase in the threshold value results in the increase of pore size dimensions and hence increase in the permeability results. The simulation results of various algorithms show that the vertical permeability obtained using Otsu's bi-level segmentation algorithm is significantly higher than the experimental hydraulic conductivity and Otsu's tri-level permeability results are under estimating the actual permeability. Hence the volumetric segmentation algorithm is considered to be predicting the vertical permeability more closely to the experimental results compared to the other algorithms.

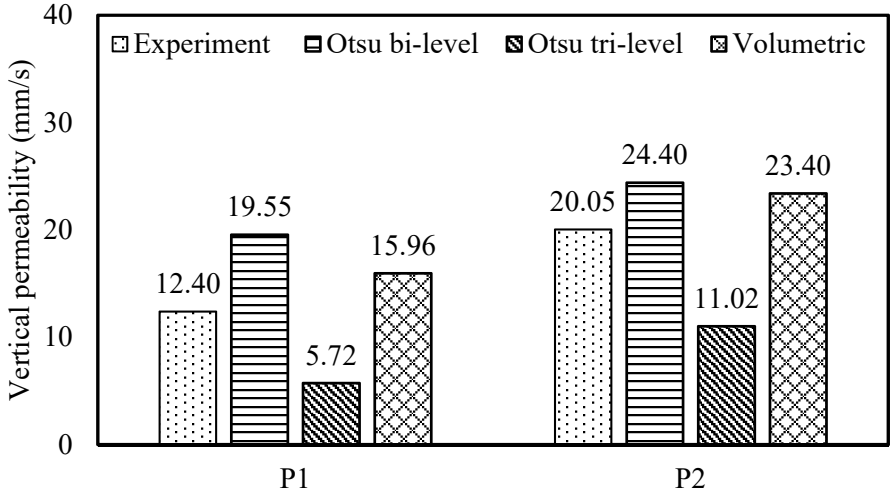

Fig.6: Vertical permeability results of thresholding techniques

Fig.7 shows the variation of permeability in the horizontal direction obtained from the simulations using various segmentation algorithms. Following the same trend observed for the vertical permeability, Otsu's bi-level horizontal permeability is higher followed by the volumetric and Otsu's tri-level simulation results. And also the simulation results of horizontal permeability are slightly higher compared with the vertical permeability results, due to the fact that the compaction of the samples was done in the vertical direction and hence the length of pore network in the horizontal direction is more than in the vertical direction.

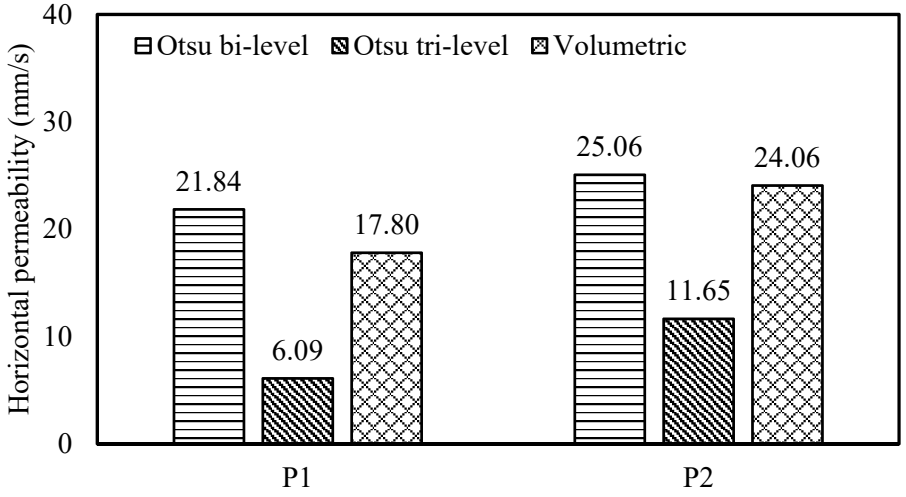

Fig.7: Horizontal permeability results of thresholding techniques

The tortuosity is the ratio of the actual length of fluid flow to the shortest distance from the top to the bottom of the sample. The anisotropic ratios and the tortuosities of the different mixtures with various segmentation algorithms were shown in Fig.8 and Fig.9. The increase in the air void threshold results in the opening of new interconnected air void channels and hence reduction in the tortuosity values. It has been observed that as the tortuosity increases, permeability also increases. A similar observation has been made in the works of Chandrappa and Biligiri (2017). Fig.10 shows the velocity streamlines in the vertical directions for the P1 sample. The lower velocity has been observed in the smaller pore channels and higher velocity in the larger pore channels. The total pressure losses in the porous domain have been observed due to the inertial effects and the geometrical features such as contraction or expansion of the pore networks.

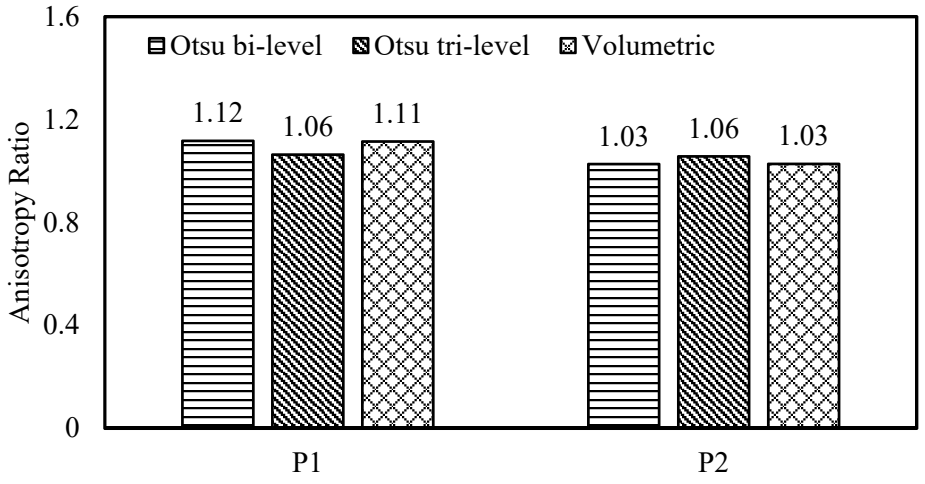

Fig.8: Influence of thresholding techniques on permeability anisotropic ratio

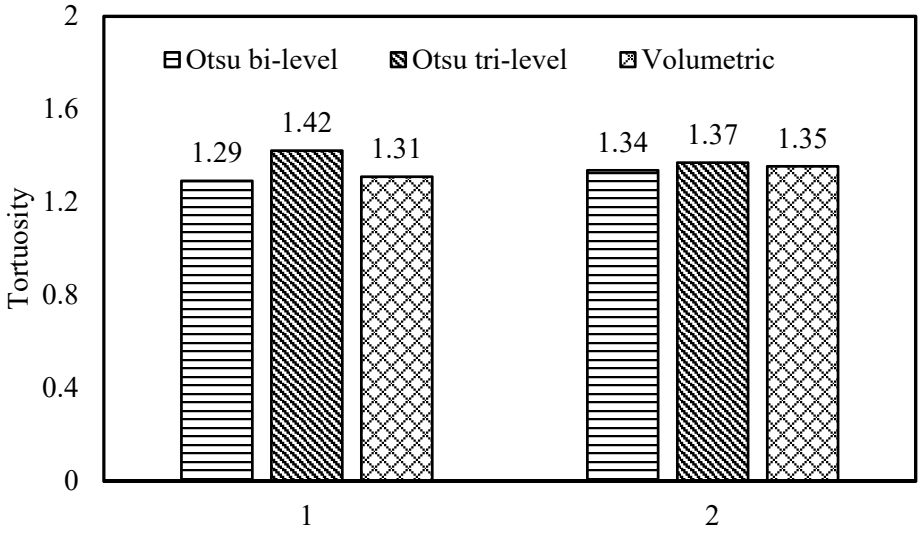

Fig.9: Influence of thresholding techniques on tortuosity

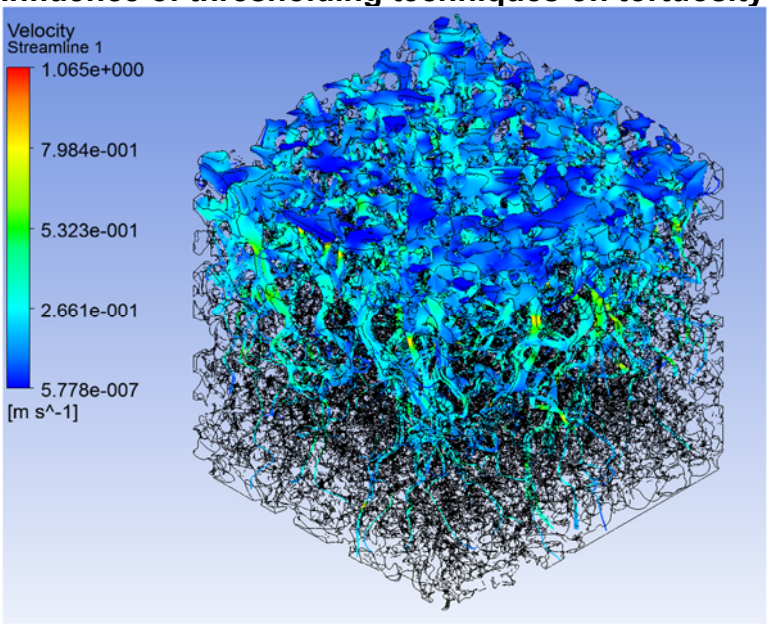

Fig.10: Velocity streamlines of pervious concrete sample

2.2 Volumetric characteristics

Fig.11 and 12 show the variation of effective porosity and isolated air voids percent for different mixtures using various segmentation algorithms. It can be seen that the amount of interconnected voids increases and the amount of isolated voids reduces with increase in threshold values due to different segmentation algorithms. Experimental results of permeability and effective porosity show that nominal maximum aggregate size has a significant influence on the permeability despite having the same effective porosity, because of its varied pore geometric properties such as the pore size distribution, tortuosity and so on. Fig.12 shows that the percentage of isolated voids is comparatively minimal because of the usage of uniformly sized aggregates and lack of fine aggregates in the mixtures. And also it has been observed that the rate of reduction in the isolated void percent with the increase in threshold values is more for mixtures with smaller nominal maximum aggregate size.

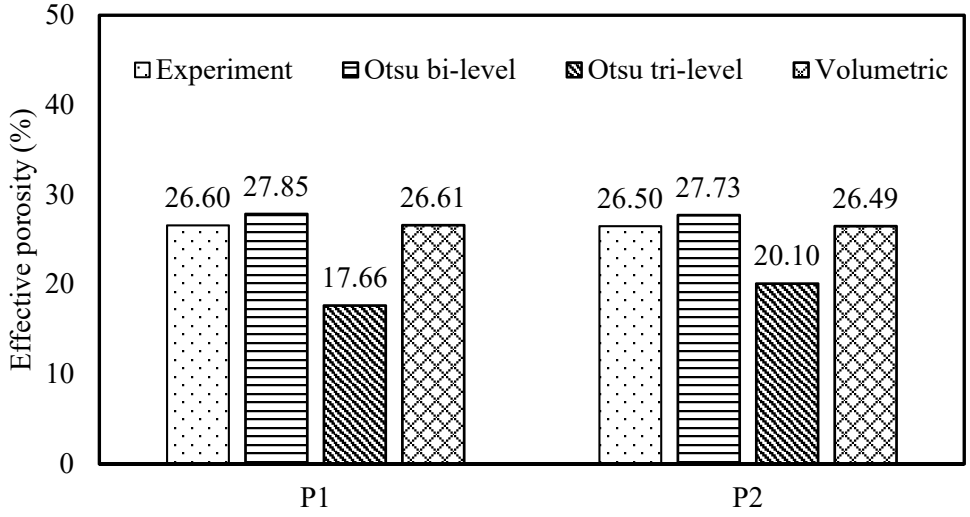

Fig.11: Influence of thresholding techniques on effective porosity (%)

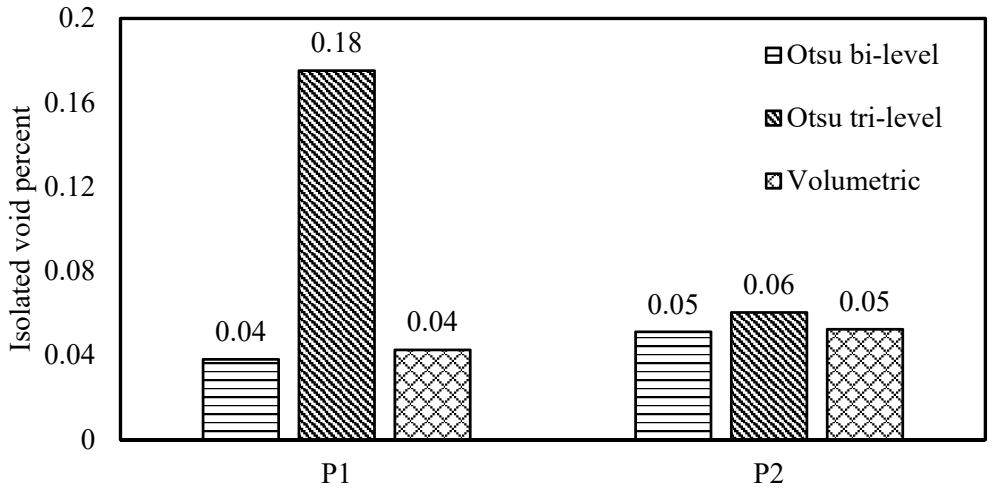

Fig.12: Influence of thresholding techniques on isolated void percent

3. CONCLUSIONS

This study analyses the influence of commonly used global thresholding algorithms on the discharge and volumetric characteristics of the pervious concrete mixtures. Internal pore network of the pervious concrete was considered using X-Ray CT scanning. Two different mixtures and three thresholding techniques were analyzed numerically using the developed finite volume based constant head permeability simulations. Based on the results of this study, the following conclusions may be drawn: (a) volumetric segmentation algorithm is considered to be predicting the permeability and effective porosity more closely to the experimental results compared to the Otsu's bi-level and tri-level algorithms; (b) Aggregate size and tortuosity have a significant influence on the permeability, despite having the same effective porosity. Overall, it is expected that the present research will help to understand the pore network characteristics of pervious concrete using non-destructive evaluation and digital image processing.

REFERENCES

Abera, K.A., Manahiloh, K.N. and Nejad, M.M., 2017. The effectiveness of global thresholding techniques in segmenting two-phase porous media. Construction and Building Materials, 142, pp.256-267.

ACI 522R-2010. Report on Pervious Concrete. American Concrete Institute.

Association of Japan Highway. 1996. Guide for Porous Asphalt Pavement. Maruzen Corporation, Tokyo, Japan.

Berengier, M.C., Stinson, M.R., Daigle, G.A. and Hamet, J.F., 1997. Porous road pavements: Acoustical characterization and propagation effects. The Journal of the Acoustical Society of America, 101(1), pp.155-162.

Chandrappa, A.K. and Biligiri, K.P., 2017. Relationships Between Structural, Functional, and X-Ray Microcomputed Tomography Parameters of Pervious Concrete for Pavement Applications. Transportation Research Record: Journal of the Transportation Research Board, (2629), pp.51-62.

Coleri, E., Harvey, J.T., Yang, K. and Boone, J.M., 2013. Micromechanical investigation of open-graded asphalt friction courses' rutting mechanisms. Construction and Building Materials, 44, pp.25-34.

Gruber, I., Zinovik, I., Holzer, L., Flisch, A. and Poulikakos, L.D., 2012. A computational study of the effect of structural anisotropy of porous asphalt on hydraulic conductivity. Construction and Building Materials, 36, pp.66-77.

Kuang, X., Ying, G., Ranieri, V. and Sansalone, J., 2015. Examination of Pervious Pavement Pore Parameters with X-Ray Tomography. Journal of Environmental Engineering, 141(10), p.04015021.

Kutay, M.E., Aydilek, A.H., Masad, E. and Harman, T., 2007. Computational and experimental evaluation of hydraulic conductivity anisotropy in hot-mix asphalt. International Journal of Pavement Engineering, 8(1), pp.29-43.

Masad, E., Al Omari, A. and Chen, H.C., 2007. Computations of permeability tensor coefficients and anisotropy of asphalt concrete based on microstructure simulation of fluid flow. Computational Materials Science, 40(4), pp.449-459.

Masad, E., Muhunthan, B., Shashidhar, N. and Harman, T., 1999. Quantifying laboratory compaction effects on the internal structure of asphalt concrete. Transportation Research Record: Journal of the Transportation Research Board, (1681), pp.179-185.

Otsu, N., 1979. A threshold selection method from gray-level histograms. IEEE transactions on systems, man, and cybernetics, 9(1), pp.62-66.

Sansalone, J., Kuang, X. and Ranieri, V., 2008. Permeable pavement as a hydraulic and filtration interface for urban drainage. Journal of irrigation and drainage engineering, 134(5), pp.666-674.

Zelelew, H.M. and Papagiannakis, A.T., 2011. A volumetrics thresholding algorithm for processing asphalt concrete X-ray CT images. International journal of pavement engineering, 12(6), pp.543-551.